UP400 Project
Report

Sources of Continuum Opacity in Hydrogen deficient stars

Submitted in partial fulfillment of the requirements for the award of the degree of

Bachelor of Science(Research)
in
Physics

Submitted by
Abhijeet Anand
Sr. No.- 11-01-00-10-91-12-1-10011

Under the guidance of

Prof. Gajendra Pandey
Indian Institute of Astrophysics, Bangalore

&

Dr. Tarun Deep Saini
Indian Institute of Science, Bangalore

Department of Undergraduate Studies
Indian Institute of Science
Bangalore - 560012, Karnataka

April 2016

Department of Undergraduate Studies

Indian Institute of Science, Bangalore

Certificate

This is to certify that work contained in the thesis entitled **“Sources of Continuum Opacity in Hydrogen deficient stars”** is a bonafide record of the project presented by **Abhijeet Anand** (Sr No.- 11-01-00-10-91-12-1-10011) during **Aug 2015 - Mar 2016** in partial fulfilment of the requirements of the degree of **Bachelor of Science(Research)** in **Physics**.

Prof. Gajendra Pandey, IIA
(Project Supervisor)

Dr. Tarun Deep Saini, IISc
(Local Guide)

Date:

Prof. K.P. Ramesh, IISc
(Subject Coordinator)

Acknowledgments

I would first like to express my deep gratitude to my project adviser Prof. Gajendra Pandey of Indian Institute of Astrophysics, Bangalore. He consistently allowed this project to be my own work, and steered me in the right direction whenever I needed it.

I am also very thankful to the Visiting Student Program and Board of Graduate Studies at IIA, who gave me the opportunity to work as a visiting student on this project and provided me the necessary resources. Many thanks to Dr. Tarun Deep Saini of Indian Institute of Science, Bangalore for being my local mentor for this project work. I also extend my thanks to my department which allowed me to pursue this project outside the institute as per my interest.

Finally, I must express my very profound gratitude to my parents and to my colleagues for providing me with unfailing support and continuous encouragement throughout my entire B.Sc(Research) course. This accomplishment would not have been possible without them. Thank you.

Abhijeet Anand
April, 2016
Indian Institute of Science, Bangalore

Contents

List of Figures

Chapter 1

Introduction

1.1 Stars

The night sky is full of tiny twinkling dots (they are much bigger than our earth !) loosely called stars. More precisely, A star is a luminous ball of gas, mostly hydrogen and helium, held together by its gravitational energy. They appear as a fixed point in the sky because of their vast distance from us, the nearest star from us is at 4.24 light-years ($\sim 4.01 \times 10^9$ km), which is very large but extremely small compared to our universe scale (~ 93 billion light-years)[17].

So how do we calculate these numbers? The only thing which we are getting from a star is light. It is the photon that is the principal source of all the information. Therefore the study of properties of starlight becomes pivotal in astronomy. We can extract many properties of stars by analyzing the incoming photons, like temperature, luminosity, age, chemical compositions, distance, and size. Since a star is a dense medium of gas, several interactions occur between emitting photons and inside material. The details of these interactions can be extracted from the stellar spectra by fitting them with black-body approximation. The best fit to their observed spectra determines their surface temperatures. We can also get some information on its life cycle. The life of a star is very dynamic. Firstly, it is formed by the collapse of dense molecular clouds then the fusion of hydrogen into helium keeps it alive for a certain period then once the fuel gets exhausted it dies giving rise to some interesting objects like white dwarfs, neutron stars, or black holes.

All these information about their physical properties and evolution are extracted by analysing the photons coming from them. The ground and space based telescopes have played a pivotal role in catching these photons and extracting information from them. In this chapter we will discuss the physics of radiation from stars in an appreciable detail.

1.1.1 Sun

In the above section, we have given a general idea of a star and photons emitting from it. Now we will focus on our own star, the Sun. Presently sun lies on the main sequence line of the HR diagram. The mean distance between earth and sun is 1 AU ($\sim 1.5 \times 10^8$ km)[8]. The mass and radius of sun is around 2×10^{30} kg and 7×10^5 km respectively[8]. Hydrogen accounts for around 75% of this mass and rest is accounted by helium along with very small quantities of heavier atoms like carbon, oxygen, neon and iron[8]. The surface temperature of sun is about 6000 K[8]. Almost entire source of energy on earth is sun, the power output of sun is 3.8×10^{33} ergs s^{-1}[8].

1.1.2 Hydrogen Deficient Stars

Typically, normal stars mainly contain hydrogen along with a significant fraction of helium, but this is not true for all stars. In fact there are stars which contain extremely low hydrogen ($< 1\%$) but a huge fraction of helium ($\sim 99\%$), these stars are called hydrogen deficient stars, first discovered in 1942[14]. Based on their chemical compositions and physical properties they are often classified in three different classes- Extreme-Helium stars (EHes), Hydrogen deficient Carbon stars (HdCs) and R Coronae Borealis stars (R CrB)[16]. In all these stars carbon is the most significant element after helium.

1.2 Radiation flow through Stellar Atmosphere

Now we move our focus towards the study of photons coming from stars, because at the end photons are the principal means by which information comes to us from the stars. The measurement on photons can provide us information on temperature and other physical quantities in the region from which the photons originated. These photons can give information of deep inner regions and outer rarefied material of stars.

1.2.1 Radiation Field in Stellar Atmosphere

The aim of studying radiative transfer in stellar atmosphere is to determine how radiation interacts with the medium as it passes through it. This interaction is mutual, because on one hand material imprints some properties on radiation and on the other hand, the material in the medium is also affected by the photons coming from deep inside the star.

An important way to describe the radiant energy is the intensity I_λ (or I_ν) which is defined as the amount of radiant energy which flows through unit area per unit time per unit wavelength (or frequency) and per unit solid angle. The units of I_λ (or I_ν) are ergs cm^{-2} sec^{-1} cm^{-1}(or Hz^{-1}) steradian^{-1}. Conservation of energy requires that $I_\lambda d\lambda = I_\nu d\nu$. This gives, $I_\lambda = I_\nu \frac{d\nu}{d\lambda}$ and since $\lambda\nu = c \Rightarrow I_\lambda = I_\nu \frac{c}{\lambda^2}$. The best example of I_λ (or I_ν) which is useful for astrophysical studies is black-body radiation. In black-body approximation the radiant intensity which is radiated *per unit frequency* from a surface at temperature T is given by Planck's radiation formula-

$$I_\nu = \frac{2\pi h\nu^3}{c^2}\frac{1}{e^{h\nu/k_BT} - 1} \tag{1.1}$$

or, intensity *per unit wavelength* is-

$$I_\lambda = \frac{2\pi hc^2}{\lambda^5}\frac{1}{e^{hc/\lambda k_BT} - 1} \tag{1.2}$$

This distribution function can be fit on the spectrum of star and the effective temperature of that star can easily be calculated. For sun effective temperature turns out to be about 6000 K.

1.2.1.1 Optical Depth

As discussed above the radiation interacts with the material in the medium, one of these interactions is absorption of radiation in the stellar atmosphere. The rate at which absorption occurs is often described by *(linear) absorption coefficient*, k_λ cm^{-1}, the subscript λ indicates that this coefficient depends on the wavelength. It also depends on temperature. In the presence of absorption (by ions, atoms or molecules), when a beam of radiation with intensity $I_\lambda(0)$ enters a uniform slab of linear thickness x, the emergent intensity is given by

$$I_\lambda(x) = I_\lambda(0)e^{-\tau} \tag{1.3}$$

where $\tau = k_\lambda x$ is a dimensionless number called the optical depth of the slab at wavelength λ. Eqn. 1.3, clearly shows that at $\tau = 1$, intensity reduces to a factor of $1/e(\approx 0.37)$ and for $\tau = 5$, the emergent intensity is attenuated below the initial value by a factor of thousand. This clearly indicates that when we see a medium where radiation is coming from a layer of depths it becomes quite hard to detect a significant fraction of radiation which comes from a gas layer of optical depth $\tau \geq 1$.

1.2.1.2 Concept of Photosphere

Now from our above definition of optical depth we can immediately see the it depends on the wavelength of light and it can characterize a particular layer of atmosphere. More formally, the increment of this optical depth $d\tau_\lambda$ is defined by $d\tau_\lambda = -k_\lambda dh$, where the negative sign shows that as we move deeper into star τ will increase. So mathematically, the local optical depth at any height h' in atmosphere is calculated by integrating from most interior $(h = 0)$ of star to the height h':

$$\tau_\lambda(h') = \int_0^{h'} k_\lambda dh \tag{1.4}$$

The location at which integral approaches to a value of order unity (for sun 2/3), is called the photosphere. Why is it important to study photosphere is because as we have discussed, it is extremely difficult to detect light coming from deeper layers of a star due to very high optical depth, so photosphere is probably the deepest layer from which we still have good chance to see what is emitted.

1.2.1.3 Rosseland Mean Optical Depth (τ_{Ross})

As from above section it is clear that τ_λ is wavelength (or frequency) dependent, so sometimes it is very useful to define a mean optical depth in astronomy. It is defined as the average of optical depth over all the wavelengths (or frequencies). Mathematically, for Planck's radiation function τ_{Ross} can be defined as-

$$\tau_{Ross} =< \tau_\lambda >= \frac{\int_0^\infty \tau_\lambda \frac{\partial I_\lambda(T)}{\partial T} d\lambda}{\int_0^\infty \frac{\partial I_\lambda(T)}{\partial T} d\lambda} \tag{1.5}$$

1.2.1.4 Concept of Model Atmosphere

It is hard to make rigorous interpretation from an observed stellar spectrum as it involves lots of physical variables. So we make our life simple by constructing a model through which we analyse the information which comes to us in the form of starlight. This model is based on known physical laws and observational data, also model is always modified with the inclusion of new data. Then we use our model to reproduce observational data and check for the consistency to know how good our model is. The model atmosphere of a star consists tables of some numbers, most prominently optical depth, temperature and pressure for an assumed chemical composition. From this model we can compute continuous opacity, line strength, fluxes and other physical variables.

1.3 Opacity

In astrophysics opacity is defined as a measure of how opaque a medium of density ρ is to the light of wavelength λ. It is given as- $\kappa_\lambda = \frac{k_\lambda}{\rho}$ and has unit cm^2g^{-1}. From units it can be seen as cross-sectional area which hinders the free passage of radiation as it propagates through 1 gm of material[8]. It plays an important role in developing the models of different layers of stellar atmosphere.

1.4 Sources of Opacity

Now the question arises that what are the sources of opacity. At the microscopic level opacity can be divided into two types depending on the physical processes involved- *line opacity* and *continuous opacity.*

1.4.1 Line Opacity

When photon passes through a medium it interacts with atoms, ions and molecules, and can be absorbed by them. The microscopic process which gives rise to line opacity is bound-bound transitions.

1.4.1.1 Bound-Bound transitions

Quantum mechanics tells us that there are discrete energy levels in an atom, in which electrons reside. The difference between different energy levels correspond to certain wavelengths. When a photon of that energy interacts with atom it is absorbed and electrons are excited to higher energy state, but they can not remain in higher energy state for indefinite time, therefore, after certain time scale they return either to their original state or some intermediate state emitting photon of that energy difference. If they come to original state they will emit photon having same energy which it had absorbed, but in random direction, but if they return to some intermediate state they will emit photons of less energy. So clearly this whole process involve two discrete energy lines that is why it is called line absorption (or emission) and causes line opacity.

It is very clear from above discussion that contribution of line opacity κ_λ^{bb} is very small at all wavelengths except those which correspond to the energy difference between two atomic levels.

1.4.2 Continuous Opacity

Above section deals with two bound orbits, but as we have seen the line opacity contributes at a given wavelength and not at all wavelengths unlike continuum opacity. So what does lead to the most of the continuum opacity, the answer is the continuous absorption of photons. The processes which are major sources of continuous opacity are- *bound-free absorption*, *free-free absorption* and *electron scattering.*

1.4.2.1 Bound-Free absorption

When photons of energy ($h\nu$) greater than ionization potential (χ_n) of an atom interact with an atom they ionize it by freeing a electron from it. The difference of energy $h\nu - \chi_n$ is imparted as the kinetic energy of that free electron which gives rise to the continuum opacity κ_λ^{bf}. It is called continuous because every photon with $h\nu > \chi_n$ will contribute to this process.

1.4.2.2 Free-Free absorption

In this process a photon is absorbed by free electrons and an ion (here, electron is not captured by ion, so it free before interaction and after interaction), which share energy and momentum of photon and emits a continuous range of photons in random direction giving rise to the free-free opacity κ_λ^{ff} and contributes to the continuous opacity.

1.4.2.3 Electron scattering

Till now we have talked about absorption of photons, but absorption is not only process which contributes to opacity, even scattering of photons by free electrons plays an important role in opacity calculation. The photons scatter from free electron without change of their energy, this is called Thomson scattering. Quantum mechanics shows that scattering cross-section is wavelength independent, so κ_{es} also contributes to the continuous opacity. Thomson cross-section of electron is very small, $\sigma_e = 6.7 \times 10^{-25}$ cm^2. So its contribution to the continuous opacity becomes important only when electron density is very high, like in hot stars.

1.4.3 Total Opacity

Now combining all the physical processes discussed above we can state the final opacity will be a sum of all these opacities (continuous and line). In a formal way we can write total opacity κ_λ^T as-

$$\kappa_\lambda^T = \kappa_\lambda^{bb} + \kappa_\lambda^{bf} + \kappa_\lambda^{ff} + \kappa_{es} \tag{1.6}$$

1.5 A Comment on the Sources of Opacity in Sun

As sun mostly contain hydrogen with helium fraction (by numbers) is one tenths of hydrogen. The major source of continuous opacity in sun is directly or indirectly hydrogen, that is H^-. In UV wavelength range H^- and He also contribute significantly towards opacity[8]. In UV wavelength range (2000-3000 Å) neutral magnesium also contributes a significant fraction[2]. In near optical wavelengths (3000-4000Å) neutral iron also enters into the picture[2]. Other metals like SiI, CI, BeII etc, don't contribute much to the solar opacity[2],[8].

1.6 Importance of Opacity Calculation

Now we will discuss the applications of opacity, which are quite broad. It helps performing chemical analysis of stars. The chemical analysis of a star brings wide information to us like what stars are made of, nuclear reactions taking place in a star, how materials are exchanging from interstellar space, their evolutionary stage and all sorts of information. The following sections will describe some applications of opacity.

1.6.1 Strength of a Line

In general, line strength is defined as total absorption associated with a spectral line, and this absorption is very closely related to the abundance. In terms of opacities *line strength* can be determined by

$$\textit{line strength} \propto \frac{\textit{line opacity}}{\textit{continuous opacity}} \tag{1.7}$$

Typically, in normal stars hydrogen directly, or indirectly is the major source of continuous opacity so spectral lines of an element E directly gives us the ratio $A_E = N_E/N_H$ without measuring hydrogen from H I line[9]. Similarly, in extreme helium stars(EHes) carbon or helium are the major source of opacity so analysis of line strength will give us the ratios $A'_E = N_E/N_C$ or $A''_E = N_E/N_{He}$. These ratios are calculated using curve-of-growth which is a log-log plot between line strength and number of absorbers.[4]

1.6.2 Abundance Analysis

Once we have obtained A_E from line strength we can calculate the mass fraction of E by following expression[9]

$$f_m(E) = \frac{\mu_E N_E}{\mu_H N_H + \mu_{He} N_{He} + ... + \mu_i N_i} \tag{1.8}$$

where $f_m(E)$ is mass fraction of element E, μ_i is atomic mass of i$^{\text{th}}$ element and N_i is number of i$^{\text{th}}$ element. For typical stars A_E is much smaller except for helium. Therefore eqn 1.8 can be reduced to

$$f_m(E) \approx \frac{\mu_E A_E}{1 + 4A_{He}} \tag{1.9}$$

Similarly in EHes[9],

$$f_m(E) = \frac{\mu_E A'_E}{\mu_H A'_H + \mu_{He} A'_{He} + ... + \mu_i A'_i} \tag{1.10}$$

Now in these stars A'_i is much smaller than $A'_{He}(\approx 100)$, therefore eqn 1.10 reduces to

$$f_m(E) \approx \frac{\mu_E A'_E}{4A'_{He}} \tag{1.11}$$

1.7 Our Problem

Now we need A'_E for our calculation which is not very easy in case of EHes, because as opacity depends on the number of absorbers, if same element is the major source of both opacities, the numbers will cancel out and we won't be able to measure the line strength spectroscopically. In normal stars N_{He}/N_H can be assumed on the basis of some astrophysical arguments, but this is not the case with N_C/N_{He} in EHes stars. So to explain when the N_C/N_{He} ratio can be or can not be directly calculated from the spectrum of H-poor star we would like to see the sources of continuous opacity in different wavelengths for different effective temperatures.

Why we are studying sources of continuous opacity at different wavelength, because once we obtain the major source of continuous opacity different wavelength regions we can easily calculate the number ratios of other elements with respect to that element (dominant contributor to the continuous opacity) by the analysis of line strength.

Chapter 2

Data Analysis

Now as we have developed our basic definitions and defined our problem, we will discuss our approach to solve the problem in this chapter. This chapter will present the detailed analysis of our approach and enable us to finally present our results in the last chapter.

2.1 Data Acquisition

The raw data for monochromatic (for UV and Optical) total continuum absorption coefficients (κ_λ) for non-hydrogenic atoms (He, Li, C, C^+, C^{++}, N^+, N^{++}, O, O^+, Na, Mg, Mg^+, Al, Al^+, Si, Si^+, Cl, Ca^+, K) in cm^2 per atom units in the temperature range 4000-48000 K, were taken from [10]. The values of these absorption coefficients for atomic systems are calculated using general photoionization cross sections derived by [3] and theory of bound-bound, bound-free and free-free transitions, which have been discussed in great detail in [11],[12],[13]. Recent calculations of total opacity using more energy levels and with improved cross-sections have been done by Opacity project[18].

2.1.1 Model Atmospheres of Hydrogen-deficient Stars

Our calculations are based on model atmospheres constructed from the classical assumptions: the energy (radiation plus convection) flux is constant, and the atmosphere consists of plane-parallel layers in hydrostatic and local thermodynamic equilibrium (LTE). We have taken models for three different effective temperatures (cooler, $T_{\mathbf{eff}}$ = 7000 K, intermediate, $T_{\mathbf{eff}}$ = 9500 K, and hotter, $T_{\mathbf{eff}}$ = 14000 K) for C/He = 1%.

2.1.1.1 Model for T_{eff} = 7000 K

For lower temperatures, We have used Uppsala line-blanketed models described by ([1]) for gravity, log g = 0.5 and C/He ratio: C/He = 1%. The abundances used for the standard grid are mainly taken from [6]. The model contains computed data for photosphere temperature in the range of 4500-16000 K, along with the tables of gas pressure, electron pressure, Rosseland mean optical depth and density gradient for given number fraction of different atoms.

2.1.1.2 Model for T_{eff} = 9500 K

To analyse cool EHe stars in intermediate temperature range (9000 K $\leq T_{eff}$ $\leq$ 11000 K), here also we have used Uppsala line-blanketed model for gravity, log g = 1.0 and C/He ratio: C/He = 1%, with other elements at fixed values as taken in T_{eff} = 7000 K model. The model contains computed data for photosphere temperature in the range of 6000-22000 K.

2.1.1.3 Model for T_{eff} = 14000 K

To analyse cool EHe stars in near hot temperature range (11000 K $\leq T_{eff}$ $\leq$ 14000 K), We have used model atmosphere calculated by STERNE code [1] [5], with gravity, log g = 2.0 and C/He ratio: C/He = 1%, with other elements at fixed values given in model itself. The model contains computed data for photosphere temperature in the range of 7000-53000 K.

2.2 Theoretical Calculations

Once we had extracted our raw data for the continuum opacities from [10], we had to extrapolate those data to our model temperatures and use it for our calculations. For UV we have taken data in the wavelength range of 2500 Å- 2800 Åand for Optical we have taken data in the wavelength range of 4500 Å- 5000 Å.

2.2.1 Extrapolation of raw data to Model Atmosphere Grids

After extracting data for continuum opacity (κ_λ) with temperature (**T**) from [10] for UV and Optical wavelengths for different atomic systems $A^{+\mathbf{m}}$ (m =

[1]Codes and model atmosphere grids can be found on http://star.arm.ac.uk/ csj/models/Grid.html

0, 1, 2), we plotted the *log* κ vs *log* T graph and fitted it with the best curve using OriginLab software (refer Appendix A and B for fitting parameters) to get a mathematical relation between these two parameters. Once we got all the required fitting parameters and mathematical relations we used them to get values for κ_λ for our model grid temperatures. All these calculations were directly performed in MS-Excel.

2.2.2 Some Mathematical Background

2.2.2.1 Conversion of units

As explained in data acquisition section, the unit for κ_λ is **cm²atom⁻¹**, but we needed κ_λ in **cm²g⁻¹**, so we used following conversion.

$$\kappa_\lambda(cm^2g^{-1}) = \frac{\kappa_\lambda(cm^2atom^{-1})\ f_i\ N_A(atoms\ mole^{-1})}{\mu_{He}(g\ mole^{-1})} \tag{2.1}$$

where, f_i is number fraction of ith element (refer Appendix D), N_A is Avoagdro's number ($= 6\times10^{23}$) and μ_{He} is the atomic mass of helium. We are using only helium mass because in these stars $\sum n_i\mu_i \approx \mu_{He}$ as number fraction of helium is close to unity.

2.2.2.2 Inclusion of Saha ionization factor

Till now we have not taken the ionization factor into account, which is not correct. As the temperature in our model atmosphere grids ranges from 5000 K to 60000 K, it is evident that not all the atoms are going to be in their neutral state, the available thermal energy at high temperatures can easily ionize (singly or even doubly) their certain fraction which can remain in equilibrium with neutral ones. In this case the κ_λ must be multiplied with the available fraction of atomic system A^{+m}, to arrive at final value of κ_λ, which will be the absolute contribution of that atomic system towards total continuous opacity. Tn statistical physics, Saha ionization factor gives the ratio of one ionized state with other as a function of temperature and pressure. Saha ionization factor is given by-

$$\frac{N_+\,N_e}{N_o} = \frac{1}{(4\pi\lambda a_o^2)^{3/2}}\,\frac{2B_+}{B_o}\exp(-I_A\lambda) \tag{2.2}$$

where $\frac{N_+}{N_o}$ is ratio of ionized ones to neural ones, N_e is electron density calculated by eqn. 2.9, $\lambda = \frac{157890}{T(K)}$, a_o is Bohr radius ($= 5.29\times10^{-9}$ cm), $\frac{B_+}{B_o}$ is the ratio of partition function of ionized to neutral, I_A is ionization potential of A^{+m} in Rydberg ($1Ry = 13.6eV$).

2.2.2.3 Calculation of Partition functions

As, clear from eqn.(2.2), for computing Saha ionization factor we require the information of partition functions of different atomic states as a function of temperature. For this we have used partition function data available in [4] as a function of temperature. Here, we plotted $log\ B$ vs θ, where θ is $\frac{5040}{T(K)}$ and fitted those data with best fitting curve using OriginLab to get a mathematical relation between these two parameters (refer Appendix C). Once we got all the constants of equation we used it to calculate the values of partition functions for our model atmosphere temperatures.

2.2.2.4 Calculation of fraction of A^{+m}

Now our task was to calculate fraction of A^{+m} at every temperature in our model atmosphere. For this we have adopted following mathematical manipulation. For every atomic system we can write,

$$\sum N_i = N_T \tag{2.3}$$

where, $\mathrm{N_i}$ is no. of atoms in $\mathrm{i^{th}}$ ionization state of a particular atomic system and $\mathrm{N_T}$ is total no. of atoms of that atomic system (and this $\boldsymbol{i}$ depends on the atomic number of the atom). For e.g. let's take a particular atom which can be neutral, singly ionized, doubly ionized and so on at some temperature. Then from eqn.(2.3) we can write-

$$N_I + N_{II} + N_{III} + ... = N_T \tag{2.4}$$

where roman subscripts I, II, III, ... denote the neutral state, singly ionized state, doubly ionized state and so on respectively. Now suppose we have to find the fraction of neutral ones, then we divide both sides by N_I and we get following

$$1 + \frac{N_{II}}{N_I} + \frac{N_{III}}{N_I} + ... = \frac{N_T}{N_I} \tag{2.5}$$

$$\Rightarrow \frac{N_I}{N_T} = \frac{1}{1 + \frac{N_{II}}{N_I} + \frac{N_{III}}{N_I} + ...} = \chi_I \tag{2.6}$$

where LHS is our required fraction (χ_I). Now RHS can be easily calculated using Saha ionization factor (eqn.(2.2)) as follows-

$$\frac{N_{II}}{N_I} = \frac{1}{N_e}\frac{1}{(4\pi\lambda a_o^2)^{3/2}}\frac{2B_{II}}{B_I}\exp(-I_1\lambda) \tag{2.7}$$

$$\frac{N_{III}}{N_{II}} = \frac{1}{N_e}\frac{1}{(4\pi\lambda a_o^2)^{3/2}}\frac{2B_{III}}{B_{II}}\exp(-I_2\lambda) \tag{2.8}$$

& so on. where N_e is given by ideal gas equation (assuming electrons to behave like ideal gas in temperature ranges of our model atmosphere grids)-

$$P_e = N_e k_B T \text{ which} \Rightarrow N_e = \frac{P_e}{k_B T} \tag{2.9}$$

The values for P_e as a function of temperature were calculated in the model itself. To get the value of $\frac{N_{III}}{N_I}$ we have just multiplied eqn.2.7 & eqn.2.8. Similarly, to get the ratio of higher ionized states to neutral ones just multiply all Saha ionization factors till the states for which we want the ratio. This is the general idea which we have adopted for all atomic systems to calculate the required fraction.

2.2.2.5 Final value of Continuum opacity(κ)

Once we got number fraction for every atomic species we multiplied this fraction with κ_λ, which we got from eqn.2.1. and this is the absolute contribution of each atomic species towards the total continuum opacity at each Rosseland mean optical depth in that wavelength.

2.2.2.6 Opacity of e^- and He^-

The above described techniques are adopted only for all atomic systems. To calculate the contribution of helium anion towards the continuum opacity we have used mathematical relation developed by [7], and opacity of electrons were calculated using methods developed by [3]. The mathematical relations are as follows-

$$\kappa(e^-) = 0.10\,\frac{P_e}{P_g}\,cm^2\,g^{-1} \text{ for He atmosphere.} \tag{2.10}$$

$$\kappa(He^-) = 4.8 \times 10^{-5}\,P_e\,cm^2\,g^{-1} \tag{2.11}$$

2.2.2.7 Calculation of number of electrons donated by A^{+m}

It is also very important to know the dominant sources of electrons which gives an idea of electron scattering and its contribution towards total continuum opacity. Now once we have calculated the fraction of singly and doubly ionized ones we can easily find the no.of electrons given by neutral and singly ionized ones. We use following argument for this. As a singly ionized atom is formed due to loss of one electron from neutral one, the fraction of singly ionized will directly give the no.of electrons given by neutral ones. Same argument follows for no.of electrons from singly ionized ones. Mathematically, this can be understood as-

$$n_e(i) = \chi_i N_e f(A) \tag{2.12}$$

where, $n_e(i)$ is no. of electrons given by atom in i^{th} ionization state, χ_i is fraction of atoms in i^{th} ionization state and f_i is the fraction of $\mathrm{i^{th}}$ atom in our model atmosphere (refer Appendix D).

Chapter 3

Results

In this chapter we are going to present our results which we have obtained from analysis. The first part will discuss the results in UV and Optical wavelengths at three different temperatures (T_{eff} = 7000 K, 9500 K & 14000 K) for our model atmospheres and second part will discuss the conclusion and future work.

3.1 Results for different Model Atmospheres

To illustrate when the C/He ratio is or is not directly determinable from the spectrum of a H-poor star, we present the results of our calculations: an investigation of the sources of continuous opacity for model atmospheres spanning the effective temperature range of interest.

3.1.1 T_{eff} = 7000 K, log g = 1.0 and C/He = 1%

At this effective temperature using our previously discussed data analysis techniques we obtained the results for total continuum opacity in UV and Optical spectrum. Once we got the values for κ_λ**(in cm^2 g^{-1})**, we plotted $log\, \kappa_\lambda$ vs $log\, \tau_{Ross}$, where τ_{Ross} is Rosseland mean optical depth (same for UV and optical wavelengths).

3.1.1.1 Ultraviolet(UV) Results

Figure 3.1, shows the run of continuous opacity at 2600 Å for the major contributors as a function of above mentioned parameter for our model atmosphere of cool stars.

It is evident from Figure 3.1 that Helium anion and neutral magnesium are the major sources of continuous opacity in the line forming regions for

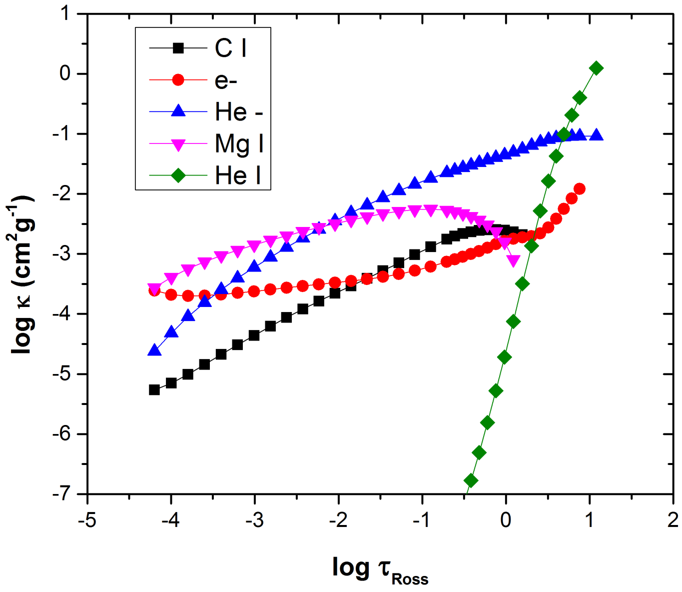

Figure 3.1: Dominant sources of continuous opacity at 2600 Å as a function of Rosseland mean optical depth (τ_{Ross}) for the model atmosphere: T_{eff} = 7000 K, log g = 1.0 and C/He = 1%

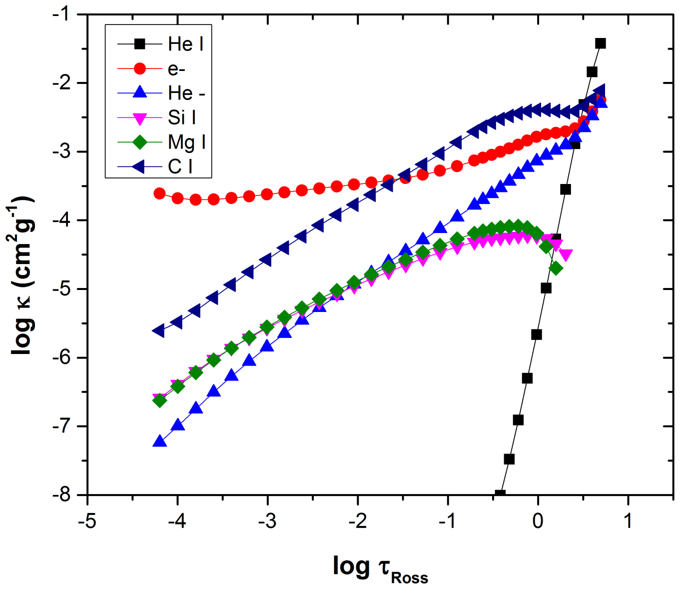

Figure 3.2: Dominant sources of continuous opacity at 5000 Å as a function of Rosseland mean optical depth (τ_{Ross}) for the model atmosphere: T_{eff} = 7000 K, log g = 1.0 and C/He = 1%

model of $T_{\text{eff}} = 7000$ K. At $log\,\tau_{Ross} = -2.06$, neutral magnesium and helium anion contribute to the continuous opacity equally. Helium anion dominates the continuous opacity for $log\,\tau_{Ross} \geq -2.1$. **e⁻** scattering also contributes significantly towards the continuous opacity for lower τ_{Ross} and neutral helium overcomes the neutral magnesium for higher τ_{Ross}.

3.1.1.2 Optical Results

Figure 3.2, shows the run of continuous opacity at 5000 Å for the major contributors as a function of above mentioned parameter for our model atmosphere for cooler stars. It can easily be seen from Figure 3.2 that electron scattering and photoionization of neutral carbon are the major sources of continuous opacity in the line forming regions for model of $T_{\text{eff}} = 7000$ K. At $log\,\tau_{Ross} = -1.6$, photoionization of neutral carbon and electron scattering contribute to the continuous opacity equally. Neutral carbon dominates the continuous opacity for $log\,\tau_{Ross} \geq -1.6$. For higher τ_{Ross} helium anion, neutral carbon, **e⁻** scattering and neutral helium contributes almost equally. Finally, neutral helium overcomes the neutral carbon for higher τ_{Ross} ($log\,\tau_{Ross} \geq 0.5$).

3.1.1.3 Dominant sources of free electrons

Since, Saha ionization factor is wavelength independent, the electron sources are same in UV and optical wavelengths. Figure 3.3, shows the dominant sources of free electrons at this effective temperature. It is quite evident from Figure 3.3 that most of the carbon is singly ionized and contributes about ninety percent of the total free electrons. The remaining ten percent of the free electrons come from oxygen. For $log\,\tau_{Ross} \geq 0$, neutral helium is the dominant source of free electrons.

3.1.2 $T_{\text{eff}} = 9500$ K, log g = 1.0 and C/He = 1%

For this intermediate effective temperature also we calculated continuum opacity and sources of free electrons using same data analysis techniques.

3.1.2.1 Ultraviolet(UV) results

Figure 3.4, shows the run of continuous opacity at 2600 Å for the major contributors as a function of Rosseland mean optical depth (τ_{Ross}) for our model atmosphere for intermediate temperature stars. It is very clear from Figure 3.4 that electron scattering is the strongest source of continuous opacity in the line forming regions for model of $T_{\text{eff}} = 9500$ K. At $log\,\tau_{Ross} = -0.5$,

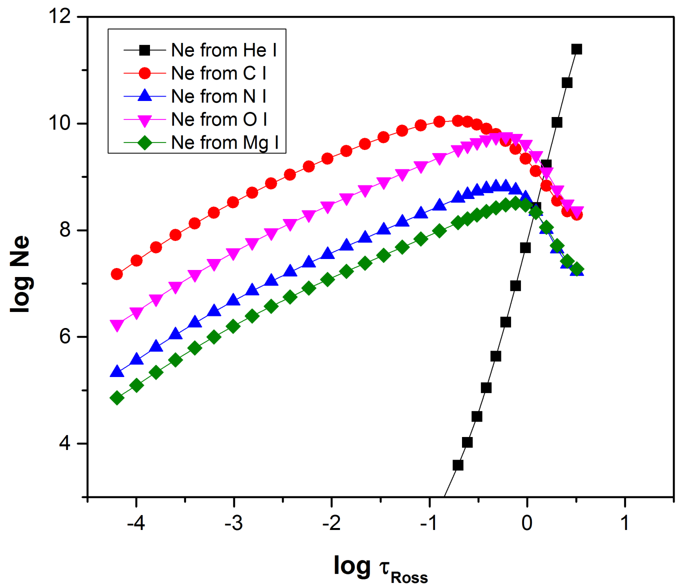

Figure 3.3: Dominant sources electrons as a function of Rosseland mean optical depth (τ_{Ross}) for the model atmosphere: T_{eff} = 7000 K, log g = 1.0 and C/He = 1%

photoionization of neutral helium and electron scattering contribute to the continuous opacity equally. In lower τ_{Ross} regions neutral carbon and neutral magnesium almost equally contributes towards continuum opacity. For higher τ_{Ross} helium anion, neutral carbon, and **e**$^-$ scattering contributes almost equally. But, neutral helium contributes far more than all other species for higher τ_{Ross} ($log\ \tau_{Ross} > -0.5$).

3.1.2.2 Optical results

Figure 3.5, shows the run of continuous opacity at 5000 Å for the major contributors as a function of Rosseland mean optical depth (τ_{Ross}) for our model atmosphere for intermediate temperature stars. We can easily see from Figure 3.5 that electron scattering and photoionization of neutral carbon are the major sources of continuous opacity in the line forming regions for model of T_{eff} = 9500 K. At $log\ \tau_{Ross} = -0.27$, photoionization of neutral carbon and electron scattering and neutral helium contribute to the continuous opacity almost equally. In lower τ_{Ross} regions neutral carbon is way smaller contributor to continuum opacity compared to **e**$^-$ scattering. For higher τ_{Ross} helium

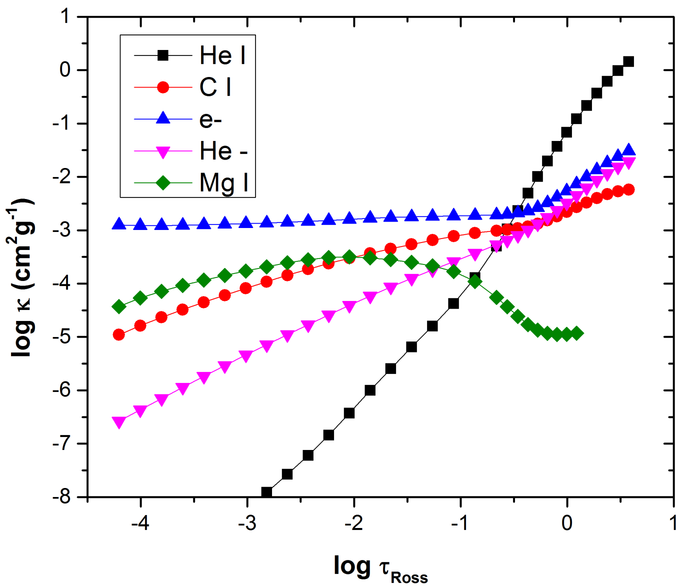

Figure 3.4: Dominant sources of continuous opacity at 2600 Å as a function of Rosseland mean optical depth (τ_{Ross}) for the model atmosphere: T_{eff} = 9500 K, log g = 1.0 and C/He = 1%

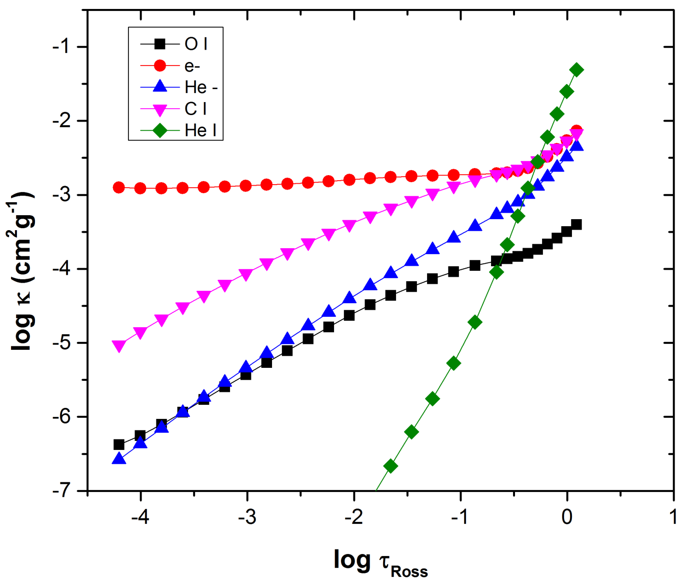

Figure 3.5: Dominant sources of continuous opacity at 5000 Å as a function of Rosseland mean optical depth (τ_{Ross}) for the model atmosphere: T_{eff} = 9500 K, log g = 1.0 and C/He = 1%

anion, neutral carbon, and **e**$^-$ scattering contributes almost equally. Again for higher τ_{Ross} ($log\, \tau > -0.5$) neutral helium dominates the total opacity. The results of our optical part are in well agreement with previous results obtained by [9]

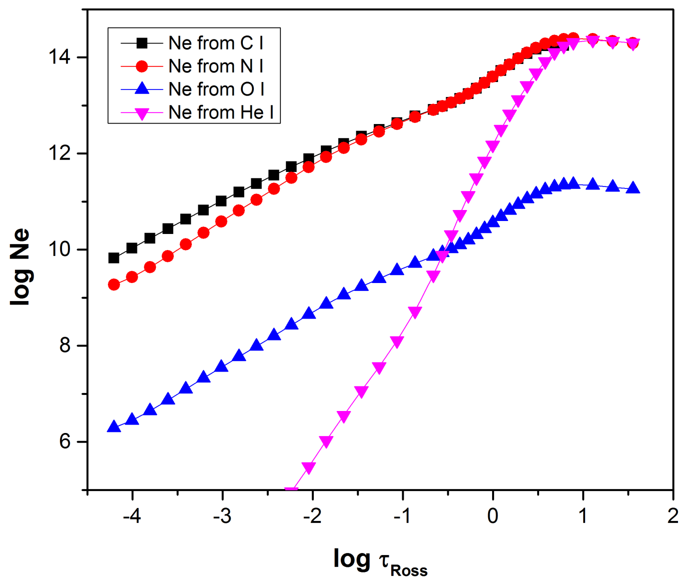

Figure 3.6: Dominant sources electrons as a function of Rosseland mean optical depth (τ_{Ross}) for the model atmosphere: T_{eff} = 9500 K, log g = 1.0 and C/He = 1%

3.1.2.3 Dominant sources of free electrons

Similar to previous model here also we have obtained the major sources of free electrons. Figure 3.6, shows the dominant sources of free electrons at T_{eff} = 9500 K. It is quite evident from Figure 3.6 that most of the carbon is singly ionized and contributes about half of the total free electrons. The remaining half of the free electrons come from neutral nitrogen. For $log\, \tau_{Ross} \geq 0.5$, neutral helium is the dominant source of free electrons. This result is also very much in agreement with previous studies done by [9].

3.1.3 T_{eff} = 14000 K, log g = 2.0 and C/He = 1%

This section will discuss our results for hot extreme helium stars in UV and optical wavelengths.

3.1.3.1 Ultraviolet(UV) results

Figure 3.7, shows the run of continuous opacity (for UV) at 2600 Å for the major contributors as a function of Rosseland mean optical depth (τ_{Ross}) for our model atmosphere of hot stars. Figure 3.7 clearly shows that electron scattering and photoionization of neutral helium are the strongest sources of continuous opacity in the line forming regions for model of T_{eff} = 14000 K. At $log\,\tau_{Ross} = -2.75$, photoionization of neutral helium and electron scattering contribute to the continuous opacity equally. In lower τ_{Ross} regions

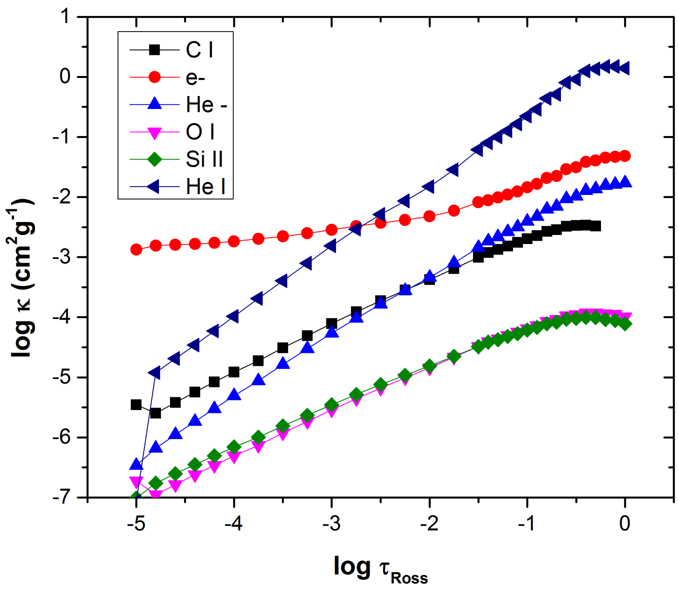

Figure 3.7: Dominant sources of continuous opacity at 2600 Å as a function of Rosseland mean optical depth (τ_{Ross}) for the model atmosphere: T_{eff} = 14000 K, log g = 2.0 and C/He = 1%

e^- scattering dominates over neutral helium, but for higher τ_{Ross} ($log\,\tau_{Ross} > -2.7$) helium dominates all species. Although neutral carbon and helium anion contribute less but they are almost equal in strength. Similar case is with singly ionized silicon and neutral oxygen.

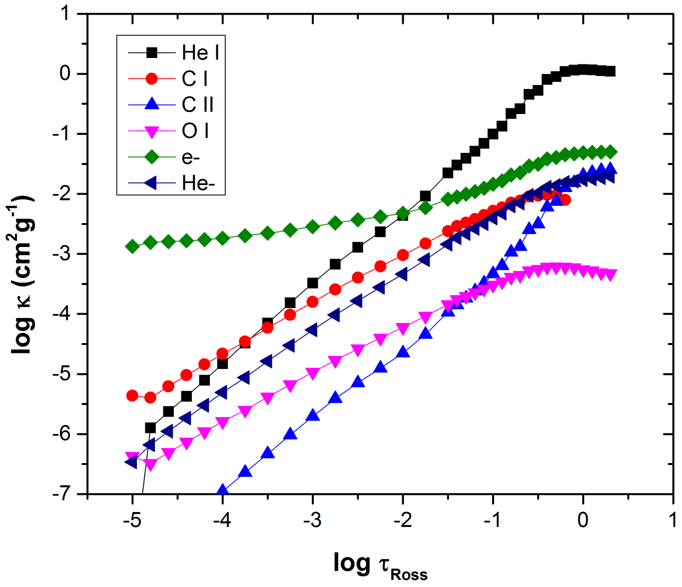

Figure 3.8: Dominant sources of continuous opacity (for Optical) at 5000 Å as a function of Rosseland mean optical depth (τ_{Ross}) for the model atmosphere: T_{eff} 14000 K, log g = 2.0 and C/He = 1%

3.1.3.2 Optical results

Figure 3.8, shows the run of continuous opacity at 5000 Å for the major contributors as a function of Rosseland mean optical depth (τ_{Ross}) for our model atmosphere of hot stars. Figure 3.8 clearly shows that electron scattering and photoionization of neutral helium are the major sources of continuous opacity in the line forming regions for model of T_{eff} = 14000 K. At $log\ \tau_{Ross} = -2.0$, photoionization of neutral helium and electron scattering contribute to the continuous opacity equally. In lower τ_{Ross} regions neutral helium is very weak contributor to continuum opacity compared to $\mathbf{e}^-$ scattering, but in this region neutral helium, helium anion and neutral carbon contributes almost equally. Here also for higher τ_{Ross} ($log\ \tau_{Ross} > -0.5$) neutral helium dominates the total opacity. This same result for optical spectrum were obtained by [9].

3.1.3.3 Dominant sources of free electrons

In same way as for other two model atmospheres, here also we have obtained the major sources of free electrons, which are same in UV and Optical spec-

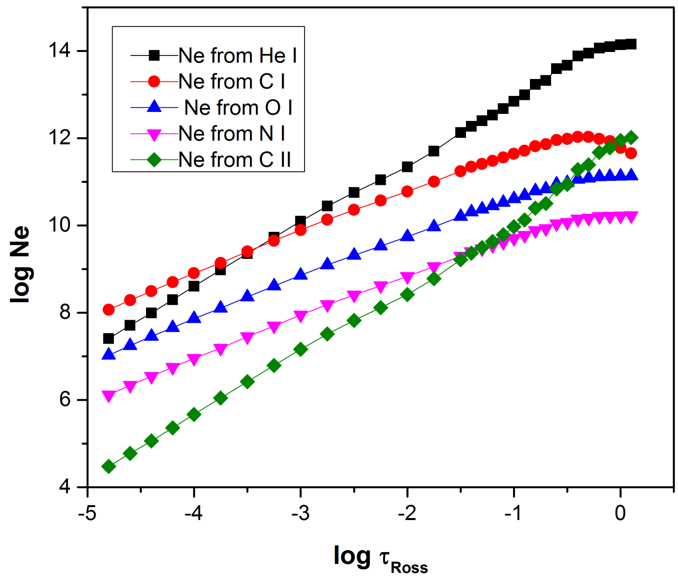

Figure 3.9: Dominant sources electrons as a function of Rosseland mean optical depth (τ_{Ross}) for the model atmosphere: T_{eff} = 14000 K, log g = 2.0 and C/He = 1%

trum, due to wavelength independence of Saha ionization factor. Figure 3.9, shows the dominant sources of free electrons at T_{eff} = 9500 K. It is well seen from Figure 3.9 that almost all the free electrons are coming from photoionization of neutral helium except for a small region for lower $log\ \tau_{Ross}$ (< -3.5). For $log\ \tau_{Ross} \geq -3.5$, neutral helium is the dominant source of free electrons, but Figure 3.9 also shows that at higher τ_{Ross} singly ionized carbon is also coming into picture. This result is also very much in good agreement with previous studies done by [9].

3.2 A General Observation

It can readily be seen that for some atomic species continuum opacity (κ_λ) of neutral ones and electrons lost (N_e) by them are decreasing for higher τ_{Ross}. This is because our model atmospheres contain a range of temperatures which correspondingly increase with τ_{Ross}. Now as the temperature becomes high enough the available thermal energy can easily ionize atoms having low ionization potential. In this case at high temperatures fraction of atoms that are in neutral state is very less compared to ionized ones and consequently these two parameters fall down. Even higher energy photons (mostly UV) can also ionize some fraction of atoms.

3.3 Conclusion

Our calculations show that for cooler stars in UV and optical metals (Mg I & C I) and He_- are the dominant sources of continuous opacity and electrons are mostly coming from C I, but as we move to intermediate temperature stars electron scattering and C I dominates the continuous opacity in optical spectrum, but in UV here also Mg I contributes a significant fraction. The sources of electrons are neutral carbon and neutral nitrogen. But at the hotter end He I and electron completely dominates the continuous opacity in both wavelengths. In this case He I is the major source of electrons.

3.4 Future Work

In this project we have done calculation of continuum opacity in UV and Optical only, but we need to calculate opacity in Infrared also to see the difference. IR calculations are important in cooler stars as UV calculations are important in hotter ones. Also the opacities have been calculated using [10], which are quite old, since then people have included more and more energy levels and calculated monochromatic opacities. A more recent calculations can be found by [18] and [15]. Now as we know the sources of continuous opacity in different wavelengths we can use this information to calculate the line strength and abundances of elements in hydrogen deficient stars.

Appendices

Appendix A

Table of Fitting Parameters of κ_λ in UV

Fitting curve for $log\,\kappa_\lambda$ vs. $log\,T$: $log\,\kappa_\lambda = K_o\,exp(-\frac{logT}{t_o}) - c_o$			
A^{+m}	K_o	t_o	c_o
He I	-58773.624	0.466	15.341
Li I	-1092.76	0.606	16.092
C I	-11249.671	0.526	15.745
N I	-14910.44	0.522	15.731
O I	-6228.441	0.597	15.345
O II	-105109.71	0.455	15.461
Si I	-11936.1	0.491	15.863
Si II	-18465.41	0.512	15.712
Na I	-379.696	0.791	16.14
Mg I	-18465.41	0.512	15.712
Mg II	-15433.3	0.521	15.29
Al I	-10055.25	0.48	16.45
Al II	-32862.32	0.486	14.855
Cl II	-14191.14	0.52	14.91
Ca II	-7544.79	0.547	15.49
K I	-214.9	0.884	15.18

All these curve were fitted with the best fitting curves with the Adj.R-Square values lying between 0.989 to 1.

Appendix B

Table of Fitting Parameters of κ_λ in Optical

Fitting curve for $log\,\kappa_\lambda$ vs. $log\,T$: $log\,\kappa_\lambda = K_o\,exp(-\frac{logT}{t_o}) - c_o$			
A^{+m}	K_o	t_o	c_o
He I	-60075.196	0.473	14.322
Li I	-3363.06	0.568	15.12
C I	-17089.32	0.502	15.141
N I	-23084.51	0.496	15.006
O I	-11450.546	0.547	14.841
Si I	-13789.5	0.484	15.33
Si II	-22165.59	0.507	15.05
Na I	-2878.76	0.580	15.320
Mg I	-13106.11	0.487	14.75
Mg II	-19554.045	0.510	14.55
Al I	-8117.73	0.493	15.78
Al II	-33832.2	0.489	13.96
Cl I	-16791.836	0.510	14.37
Ca II	-13088.014	0.521	14.72
K I	-1501.067	0.621	14.91

Here also, these curve were fitted with the best fitting curves with the Adj.R-Square values lying between 0.99 to 1.

Appendix C

Table of Fitting Parameters of Partition Functions

Fitting curve for $log\ B$ vs. θ: $log\ B = K_o exp(-\frac{\theta}{t_o}) + c_o$, $\theta = 5040/T(K)$			
A^{+m}	K_o	t_o	c_o
Li I	9.07	0.155	0.303
C I	0.479	0.240	0.952
C II	0.553	0.104	0.771
C III	2.048	0.075	-8.36×10^{-5}
N I	1.608	0.159	0.603
N II	0.298	0.252	0.936
O I	0.421	0.198	0.940
O II	1.6	0.118	0.602
Si I	1.731	0.179	0.945
Si II	0.588	0.149	0.745
Si III	2.076	0.075	-8.3×10^{-3}
Na I	21.486	0.119	0.315
Mg I	16.68	0.113	0.0054
Mg II	2.222	0.089	0.301
Al I	9.9	0.104	0.766
Al II	4.48	0.09	-6.56×10^{-5}
Al III	0.675	0.074	0.301
Cl I	0.225	0.285	0.73
Cl II	0.245	0.611	0.875
Ca I	19.91	0.149	0.029
Ca II	0.92	0.398	0.284
K I	17.84	0.141	0.323

Here also, these curve were fitted with the best fitting curves with the

Adj.R-Square values lying between 0.99 to 1. As He II is hydrogen like atom, its partition function is given as $B_{He^+} = 2n^2$ and as $n = 1 \Rightarrow B_{He^+}$ is 2. For Na II, Mg III, Ca III & K II we have taken $log\ B = 0.000$.

Appendix D

Table of Abundances

Assumed Abundances in Model Atmosphere		
Element (E)	log A	N_E/N_T
He	11.53	9.88×10^{-1}
Li	3.54	1.00×10^{-8}
C	9.54	9.98×10^{-2}
N	7.59	1.12×10^{-4}
O	8.5	8.85×10^{-4}
Si	7.09	3.54×10^{-5}
Na	5.86	2.10×10^{-6}
Mg	7.12	3.80×10^{-5}
Al	6.01	2.90×10^{-6}
Cl	6.14	3.90×10^{-6}
Ca	5.9	2.29×10^{-6}
K	5.74	1.58×10^{-6}

where, log A gives the abundance with respect total number of atoms. From log A, we calculate number fraction of element E, by following expression-

$$\frac{N_E}{N_T} = 10^{(log\ A - 11.54)} \tag{D.1}$$

References

[1] Asplund, M., Gustafsson, B., Kiselman, D., Eriksson, K., 1997a, *A&A*, **318**, 521.

[2] Bell, Roger A., Balachandran, Suchitra C., Bautista, Manuel., 2001, *ApJ*, **546**, L65.

[3] Burgess, A., Seaton, M.J., 1960. *MNRAS,* **120**, 121.

[4] Gray, David F., The observation and analysis of stellar photospheres, 2005, Cambridge Univ. Press.

[5] Jeffery, C. S., Heber U., 1992, A&A, **260**, 133.

[6] Lambert, D. L., Rao, N. K., 1994, JAA, **15**, 47.

[7] McDowell, M.R.C., Myerscough, V.P., 1966, *MNRAS,* **132**, 457.

[8] Mullan, Dermott J., Physics of the Sun: A First Course, 2010, CRC Press.

[9] Pandey, G., Rao, N.K., Lambert, D. L., Jeffery, C. S. Asplund M., 2000, *MNRAS,* **1**, 000.

[10] Peach, G., 1970. *Mem. R. astr. Soc.,* **73**, 1.

[11] Peach, G., 1967. *Mem. R. astr. Soc.,* **71**, 1.

[12] Peach, G., 1967. *Mem. R. astr. Soc.,* **71**, 29.

[13] Peach, G., 1965. *MNRAS,* **71**, 13.

[14] Popper, D.M., 1942,*PASP*, **54**, 160.

[15] Seaton, M. J., Yan, Y., Mihalas, D., Pradhan, A. K., 1994, *MNRAS*, **266**, 805.

[16] Warner, Brian., 1967,*MNRAS*, **137**, 119.

[17] https://en.wikipedia.org/wiki/Star.

[18] http://opacity-cs.obspm.fr/opacity/index.html